

Discovering novel order parameters in the Potts model: A bridge between machine learning and critical phenomena

Yi-Lun Du,^{1,*} Nan Su,^{2,†} and Konrad Tywoniuk^{3,‡}

¹*Shandong Institute of Advanced Technology, Jinan 250100, China*

²*Frankfurt Institute for Advanced Studies, 60438 Frankfurt am Main, Germany*

³*Department of Physics and Technology, University of Bergen, Postboks 7803, 5020 Bergen, Norway*
(Dated: May 12, 2025)

Machine learning (ML) models trained on Ising spin configurations have demonstrated surprising effectiveness in classifying phases of Potts models, even when processing severely reduced representations that retain only two spin states. To unravel this remarkable capability, we identify a family of novel alternative order parameters for the $q = 3$ and $q = 4$ Potts models on a square lattice, constructed from the occupancies of secondary and minimal spin states rather than the conventional dominant-state order parameter. Through systematic finite-size scaling analyses, we demonstrate that these observables—including a magnetization-like observable derived from a reduced spin representation—accurately capture critical behavior, yielding critical temperatures and exponents consistent with established theoretical predictions and numerical benchmarks. Furthermore, we rigorously establish the fundamental relationships between these alternative order parameters, demonstrating how they collectively encode criticality through different aspects of spin configurations. Our results provide a thermodynamic basis for ML’s success in reduced representations. This work bridges data-driven ML approaches with fundamental statistical mechanics, showing that criticality in Potts systems can be encoded in more compact, non-traditional forms, and opens avenues for discovering analogous order parameters in broader spin systems.

I. INTRODUCTION

Recent advances in machine learning (ML) have profoundly impacted the scientific studies [1–3]. In condensed matter and statistical physics, ML has enabled tasks such as phase classification [4–14], topological feature identification [12, 13, 15–18], ground-state searching [19–22], and accelerated Monte-Carlo sampling [23–27]. Central to these applications is the ability of artificial neural networks (ANNs) to recognize patterns in high-dimensional data, such as spin configurations generated via Monte-Carlo simulations. Both supervised [8, 9, 28] and unsupervised [4–7] approaches have proven successful in analyzing such simulation data. The Ising model has emerged as a key testbed for these ML techniques due to its simplicity and well-characterized critical behavior, with ANNs successfully determining its critical temperature and exponents [5, 8, 29–31], establishing a paradigm for data-driven investigations of phase transitions.

Despite these successes, the “black-box” nature of ANNs poses a significant challenge: their decision-making processes and learned features often lack interpretability, limiting both reliability and generalizability. Recent work has begun addressing these limitations by examining the underlying mechanisms behind critical temperature determination [32] and exploring generalization in ML applications [33, 34]. These concerns become particularly salient when extending ML models to systems beyond their training data, such as from the Ising model to Potts model—a generalization of the former from $Z(2)$ to $Z(q)$ symmetry. The Potts model serves as an ideal framework to explore the applicability [35–41] and generalizability [42–46] of the trained networks across physical systems, as its q -component spin configurations differ fundamentally from the binary Ising spins. Furthermore, the universality classes of the Potts model also govern the phase transition of $SU(N)$ gauge theories, so this line of study also has direct impact to high energy physics.

This fundamental difference necessitates careful reconciliation between Ising and Potts spin representations when studying generalizability. Recent work has proposed various procedures to bridge this gap [42–45]. In Ref. [45], a mapping procedure of spin configuration from q -components to first 2-components, i.e. $\{1, 2, 3, \dots, q\} \mapsto \{-1, 1, 0, \dots, 0\}$, is employed without loss of generality. Remarkably, ANNs trained on Ising data can classify phases and extract critical exponents from these mapped Potts configurations for different q value and lattice geometry [45], suggesting that critical properties persist in these simplified spin representations. Yet the fundamental reasons for this success, specifically what physical quantities the networks actually learn from reduced configurations, remains unresolved.

* yilun.du@iat.cn

† nansu@fias.uni-frankfurt.de

‡ konrad.tywoniuk@uib.no

In this work, we address this gap by identifying alternative order parameters for the Potts model that encode the model's critical behavior. Building on established evidence that ANNs trained on Ising model configurations effectively learn magnetization-like features [8, 32], we hypothesize that when applied to reduced Potts model representations, these networks similarly extract order parameters analogous to magnetization - specifically, quantities proportional to the sum of all spin values. Furthermore, we propose a family of observables derived not only from dominant spin state (conventional order parameter) but also from secondary and minimal occupancies, revealing a hidden encoding of critical properties. Through finite-size scaling (FSS) analyses of $q = 3$ and $q = 4$ Potts models on square lattices, we demonstrate that these alternative order parameters—including a magnetization analog matching the form of Z_5 clock model order parameters [47] and representing a static version of dynamic Potts order parameters [48]—accurately reproduce established critical temperatures and exponents. Our results provide a thermodynamic foundation for ML's empirical success, demonstrating that criticality in Potts systems can be robustly encoded in more compact, non-traditional forms.

This paper is organized as follows: Sec. II gives a brief introduction to the Ising and Potts models, detailing their conventional order parameters and Monte-Carlo simulation methodology. In Sec. III, we propose novel alternative order parameters, rigorously validate their critical behavior through finite-size scaling, and elucidate their connection to ML-compatible mappings of spin configurations. Finally, in Sec. IV we summarize our key findings and discuss their implications for both statistical physics and machine learning applications. Complementary finite-size scaling analyses supporting our main results are presented in the Appendix.

II. THE ISING AND POTTS MODELS

The Hamiltonian of the ferromagnetic nearest-neighbor Ising model with vanishing external magnetic field reads

$$H_{\text{Ising}} = -J \sum_{\langle i, j \rangle} \sigma_i \sigma_j, \quad (1)$$

where $\sigma \in \{-1, 1\}$ denoting the spin configurations, $\langle i, j \rangle$ stands for the nearest neighbouring sites i and j , and the coupling J is set to unity. This system undergoes a second-order phase transition at the critical temperature $T_c = 2/\ln(1 + \sqrt{2}) \approx 2.269$. The order parameter is the magnetization per site: $M = |\Sigma_i \sigma_i|/N$, where N is the total number of spins. Below T_c , the system is ordered with $\langle M \rangle > 0$, while above T_c , the system is disordered with $\langle M \rangle = 0$.

The Potts model is a generalization of the Ising model from two to q states. The Hamiltonian of ferromagnetic Potts model reads

$$H_{\text{Potts}} = -J \sum_{\langle i, j \rangle} \delta_{\text{Kr}}(\sigma_i, \sigma_j), \quad (2)$$

where $\sigma \in \{1, \dots, q\}$ and the Kronecker delta δ_{Kr} evaluates to 1 if $\sigma_i = \sigma_j$ and 0 otherwise. For $q = 2$, this reduces to the Ising model up to a factor of 2 in the coupling constant. The Ising model and Potts model can be defined for different lattice geometries and dimensions. For two-dimensional ($d = 2$) q -state Potts model on a square lattice, the critical temperature $T_c = 1/\ln(1 + \sqrt{q})$ [49], with second-order phase transitions for $q \leq 4$ [50] and first order for $q \geq 5$ [51], see also the review [52] and references therein. In this work, we restrict our attention to $q \leq 4$ Potts model on a square lattice in two dimensions ($d = 2$). The order parameter for q -state Potts model is usually defined as

$$M_{\text{Potts}} = \frac{q \frac{\max\{N_i\}}{N} - 1}{q - 1}, \quad (3)$$

where N_i ($i = 1, 2, \dots, q$) is the number of spins in state i in the configuration of the Potts model, and is referred to as the multiplicity of state i . $N = \sum_i^q N_i$ is the total number of spins and equals to L^d with L the lattice size. This definition actually makes use of the occupancy of the most numerous state in each configuration $\max\{N_i\}/N$. For $q = 2$, it is equivalent to the conventional order parameter of the Ising model, i.e., the global magnetization

$$M_{\text{Ising}} = \frac{|N_1 - N_2|}{N}, \quad (4)$$

here N_1 and N_2 are referred to as the number of spins -1 and $+1$, respectively. N_1/N and N_2/N are not independent and we actually have

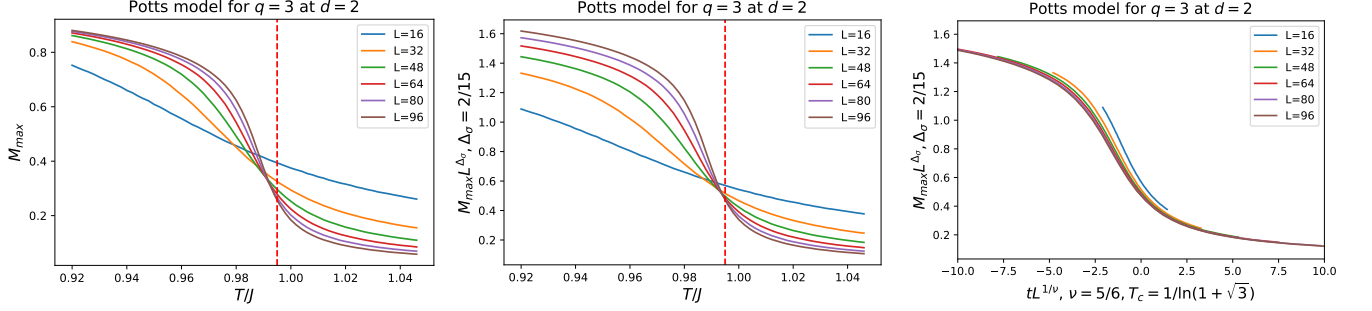


FIG. 1. (Color online) (Left) Order parameter M_{\max} as a function of temperature T for the $q = 3$ Potts model on a square lattice with six different system sizes L . (Middle) Scaled order parameter $M_{\max} L^{\Delta_\sigma}$ versus T , with curves intersecting near the theoretical critical temperature T_c , marked by the red vertical dashed line. (Right) Scaled order parameter $M_{\max} L^{\Delta_\sigma}$ against the rescaled temperature $tL^{1/\nu}$, demonstrating data collapse consistent with finite-size scaling.

$$\frac{\max\{N_i\}}{N} = \frac{|N_1 - N_2|}{2N} + \frac{1}{2}. \quad (5)$$

Since the definition of M_{Potts} in Eq. (3) contains the maximal occupancy, in the following we use M_{\max} to label M_{Potts} to distinguish the alternative order parameters we will propose for the Potts model.

In our Monte Carlo simulations, we use the Swendsen-Wang algorithm [53] by the package in GitHub [54] to generate spin configurations with periodic boundary conditions. Each lattice is first equilibrated for 1000 cluster updates, after which spin configurations are sampled every k cluster updates, where k is the number of updates to decorrelate the current update with previous ones for each lattice size setup. A total of 64 sampling temperatures T are used in Monte Carlo simulations with an interval $0.002J$ and the critical temperature T_c is covered. For lattice of size $L \times L$ with $L = \{16, 32, 48, 64, 80, 96\}$, 100,000 samples are generated for each temperature.

Taking $q = 3$ Potts model on a square lattice ($d = 2$) as an example, we show the simulation results of the order parameter, i.e., the ensemble average of $M_{\max}(T)$ for different lattice size L in Fig. 1. Theoretically, $\bar{M}_{\max}(T)$ satisfies that $\bar{M}_{\max} = 0$ when $T > T_c$ and $\bar{M}_{\max} > 0$ when $T < T_c$. The Monte-Carlo lattice simulation shows the finite-size effect for this picture in the left panel. Near T_c , the order parameter \bar{M} in general satisfy $\bar{M}(L, T) = L^{-\Delta_\sigma} \tilde{m}(tL^{1/\nu})$, where $t = (T - T_c)/J$, $\nu = 5/6$ and $\Delta_\sigma = 2/15$ are the critical exponent and scaling dimension [52]. With the finite-size scaling procedure, the plot $\bar{M}(L, T)L^{\Delta_\sigma} - T$ with different lattice size L shows a crossing point at T_c and the plot $\bar{M}(L, T)L^{\Delta_\sigma} - tL^{1/\nu}$ with different L presents a data collapse on top of each other, as shown in the middle and right panel of Fig. 1, respectively.

III. ALTERNATIVE ORDER PARAMETERS FOR POTTS MODEL

Ref. [45] demonstrated a remarkable capability of ANNs in classifying phases across different spin models. ANNs were first trained using Ising model spin configurations across various temperatures to classify phases. Then these Ising-trained ANNs were successfully applied to classify phases in Potts models of the same lattice size. To bridge the fundamental difference in spin representations between these models (binary spins in Ising versus q -state spins in Potts), an elegant mapping procedure $\{1, 2, 3, \dots, q\} \mapsto \{-1, 1, 0, \dots, 0\}$ was introduced for $q \leq 7$, where only first two spin states are preserved while others are set to zero. This mapping maintained all essential physics while providing compatibility with the Ising-trained networks. Remarkably, these ANNs not only accurately classified Potts model phases but also correctly extracted critical exponents for $q \leq 4$ cases. The success of this mapping procedure inspired our current investigation into alternative order parameters that might underlie this surprising generalizability.

A. $q = 3$ Potts model on a square lattice

For the $q = 3$ case, the mapping of three spin components takes the form,

$$\{1, 2, 3\} \mapsto \{-1, 1, 0\}, \quad (6)$$

where we keep the first two components and ignore the third one by setting it as zero. Building on the established understanding that ANNs trained on Ising models learn to detect magnetization patterns, i.e., the sum of all spin values. we define a corresponding order parameter for the mapped Potts model:

$$M_{\text{map}} = \frac{|N_1 - N_2|}{N}. \quad (7)$$

M_{map} represents a natural generalization of order parameter for the Ising model. For $q = 2$ Potts model, M_{map} is equivalent to M_{max} in Eq. (3). Our finite-size scaling analysis (shown in Appendix Fig. A1) demonstrates that M_{map} successfully captures critical behavior using the known critical exponents ν and Δ_σ , confirming its validity as an order parameter. In this work, we are concerned with the static critical properties of Potts model in equilibrium and notably M_{map} could be viewed as a static version of the alternative order parameter for Potts model at an early stage of the time evolution of dynamics at non-equilibrium [48]. It's also worth noting that M_{map} has the same form of the order parameter for Z_5 model, *aka* 5-state clock model [47].

To relate M_{max} and M_{map} theoretically, we can make use of the minimal state occupancy in each configuration $\min\{N_i\}/N$. As we know, $\min\{N_i\}/N$ also tends to $1/q$ when $T > T_c$. While at low T , this occupancy is suppressed by the dominant state. So here we construct an observable M_{min} by replacing the occupancy of the most state in each configuration $\max\{N_i\}/N$ in Eq. (3) with the least one, $\min\{N_i\}/N$:

$$M_{\text{min}} = \frac{q \frac{\min\{N_i\}}{N} - 1}{q - 1}. \quad (8)$$

We assume that in one configuration, the occupancy of three states descends as a, b, c . With the $Z(3)$ symmetry, we could have 6 cases of how these three occupancies are assigned to these 3 states. After smearing a specific state of these three ones with the mapping procedure, the average M_{map} of these 6 configurations equals $2(a - c)/3$. Due to that $M_{\text{max}} = (3a - 1)/2$ and $M_{\text{min}} = (3c - 1)/2$ as in Eqs. (3) and (8), we derive the fundamental relationship :

$$\bar{M}_{\text{map}} = \frac{4}{9}(\bar{M}_{\text{max}} - \bar{M}_{\text{min}}). \quad (9)$$

where the line signifies the ensemble average. This is also confirmed numerically in Fig. 2, where M_{max} , M_{min} and M_{map} as functions of temperature T with lattice size $L = 80$ are shown and the curve of M_{map} labeled with red triangles and that of $\frac{4}{9}(M_{\text{max}} - M_{\text{min}})$ labeled with gray dots collapse on top of each other. The fluctuations of M_{map} are much larger than those of $\frac{4}{9}(M_{\text{max}} - M_{\text{min}})$, mainly due to the fluctuations between those 6 configurations for M_{map} .

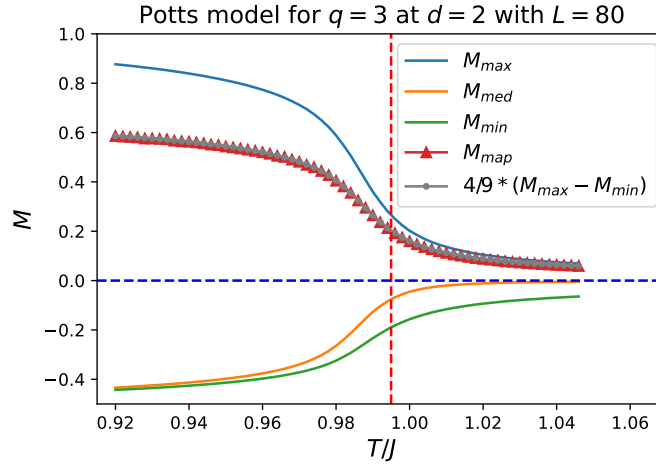


FIG. 2. (Color online) Alternative order parameters M_{max} , M_{med} , M_{min} and M_{map} as functions of temperature T for the 3-state Potts model at $d = 2$, simulated on a square lattice of size $L = 80$. The relation $M_{\text{map}} = \frac{4}{9}(M_{\text{max}} - M_{\text{min}})$ is confirmed by the overlap of the curves. The blue horizontal dashed line marks zero to indicate the sign, while the red vertical dashed line denotes the theoretical critical temperature T_c .

With Eq. (9), we can conjecture that M_{min} could also serve as an alternative order parameter. For $q = 3$, we also have the medium state for each configuration and therefore define

$$M_{\text{med}} = \frac{q \frac{\text{medium}\{N_i\}}{N} - 1}{q - 1}. \quad (10)$$

Due to the constraint that $M_{\max} + M_{\text{med}} + M_{\min} = 1$, only two of them are independent. We conjecture that M_{med} could serve as an alternative order parameter as well. The temperature dependence of these candidate order parameters and their associated finite-size scaled results for $|M_{\min}|$ and $|M_{\text{med}}|$ are shown for better visualization, respectively, in Figs. A2 and A3 in Appendix with the known values of ν and Δ_σ , which validates that M_{\min} and M_{med} could also serve as alternative order parameters.

With the FSS procedure [55], we locate the critical temperature and extract the critical exponents for all these order parameters M_{\max} , M_{med} , M_{\min} and M_{map} as detailed in Tab. I. They agree with the theoretical values very well and we conclude that all occupancies of these states along with the magnetization-like quantity M_{map} can serve as order parameters for $q = 3$ Potts model. It would be interesting to check if this conclusion is valid for other q -state Potts models. In Ising model, we have two occupancies and only one is independent, which is a trivial case. So we will turn to $q = 4$ Potts model in next subsection.

Order parameter	T_c	Δ_σ	ν
M_{\max}	0.9935(1)	0.137(6)	0.84(2)
M_{\min}	0.9931(1)	0.139(4)	0.83(6)
M_{med}	0.9940(2)	0.138(16)	0.84(5)
M_{map}	0.9942(4)	0.134(16)	0.84(10)
Theoretical value	$1/\ln(1 + \sqrt{3}) \sim 0.9950$	$2/15 \sim 0.1333$	$5/6 \sim 0.8333$

TABLE I. Critical properties of the 3-state Potts model at $d = 2$ on a square lattice, obtained using the alternative order parameters M_{\max} , M_{med} , M_{\min} and M_{map} . The critical temperature T_c , scaling dimension Δ_σ , and critical exponent ν , along with their standard errors, are estimated via finite-size scaling within the interval $T \in (0.920, 1.046)$ with step size $\Delta T = 0.002$. Theoretical values from the literature are included for comparison.

B. $q = 4$ Potts model on a square lattice

For the $q = 4$ case, besides the most and least states, we also have the second most and second least states for each configuration, therefore we define

$$M_{\max}^{\text{sec}} = \frac{q \frac{\text{secmax}\{N_i\}}{N} - 1}{q - 1}, \quad (11)$$

$$M_{\min}^{\text{sec}} = \frac{q \frac{\text{secmin}\{N_i\}}{N} - 1}{q - 1}. \quad (12)$$

In the mapping procedure for $q = 4$ case [45], only first two states are kept in the configuration without loss of generality,

$$\{1, 2, 3, 4\} \mapsto \{-1, 1, 0, 0\}, \quad (13)$$

and M_{map} is defined the same as in Eq. (7). As the analysis for 3-state Potts model, we assume that in one configuration, the occupancy of four states descends as a, b, c, d . With the $Z(4)$ symmetry, we could have 24 cases of how these four occupancies are assigned to these 4 states. After smearing two specific states of these four ones with the mapping procedure, the average M_{map} of these 24 configurations equals $(3(a - d) + (b - c))/6$. Due to that $M_{\max} = (4a - 1)/3$ and $M_{\min} = (4d - 1)/3$ as in Eqs. (3) and (8) and $M_{\max}^{\text{sec}} = (4b - 1)/3$, and $M_{\min}^{\text{sec}} = (4c - 1)/3$ as in Eqs. (11) and (12), we derive the fundamental relationship

$$\bar{M}_{\text{map}} = \frac{1}{8}(3(\bar{M}_{\max} - \bar{M}_{\min}) + \bar{M}_{\max}^{\text{sec}} - \bar{M}_{\min}^{\text{sec}}), \quad (14)$$

where the line signifies the ensemble average. This is also confirmed numerically in Fig. 3, where M_{\max} , M_{\max}^{sec} , M_{\min}^{sec} , M_{\min} and M_{map} as functions of temperature T with lattice size $L = 80$ are shown and the curve of M_{map} labeled with red triangles and that of $\frac{1}{8}(3(M_{\max} - M_{\min}) + M_{\max}^{\text{sec}} - M_{\min}^{\text{sec}})$ labeled with gray dots collapse on top of each other. Again, it's worth noting that the fluctuations of M_{map} are much larger than those of $\frac{1}{8}(3(M_{\max} - M_{\min}) + M_{\max}^{\text{sec}} - M_{\min}^{\text{sec}})$, which is mainly due to the fluctuations between those 24 configurations for M_{map} .

The temperature dependence of M_{\max} , $-M_{\max}^{\text{sec}}$, $|M_{\min}^{\text{sec}}|$, $|M_{\min}|$ and M_{map} and their associated finite-size scaled results are shown for better visualization, respectively, in Figs. A4-A8 in Appendix with the known Monte-Carlo

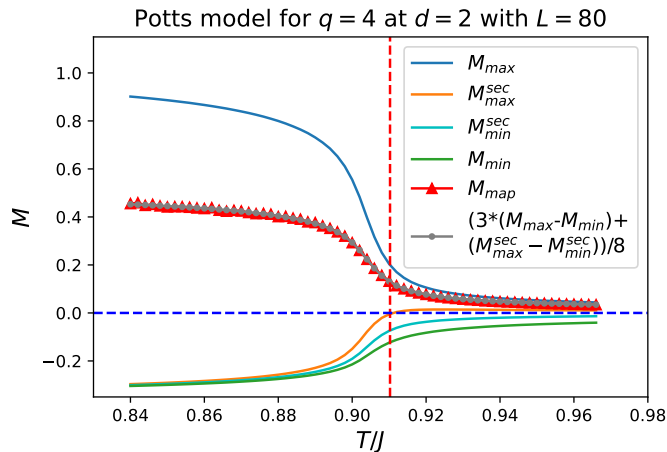


FIG. 3. (Color online) Alternative order parameters M_{\max} , M_{\max}^{sec} , M_{\min}^{sec} , M_{\min} and M_{map} as functions of temperature T for the 4-state Potts model at $d = 2$, simulated on a square lattice of size $L = 80$. The relation $M_{\text{map}} = \frac{1}{8}(3(M_{\max} - M_{\min}) + M_{\max}^{\text{sec}} - M_{\min}^{\text{sec}})$ is confirmed by the overlap of the curves. The blue horizontal dashed line marks zero to indicate the sign, while the red vertical dashed line denotes the theoretical critical temperature T_c .

Order parameter	T_c	Δ_σ	ν
M_{\max}	0.90948(8)	0.128(12)	0.723(27)
M_{\max}^{sec}	0.90965(8)	0.128(42)	0.724(5)
M_{\min}^{sec}	0.90945(8)	0.128(15)	0.721(3)
M_{\min}	0.90916(8)	0.129(8)	0.72812(1)
M_{map}	0.9094(2)	0.128(22)	0.722(13)
Theoretical value	$1/\ln(1 + \sqrt{4}) \sim 0.9102$	0.128*	0.722*

TABLE II. Critical properties of the 4-state Potts model at $d = 2$ on a square lattice, obtained using the alternative order parameters M_{\max} , M_{\max}^{sec} , M_{\min}^{sec} , M_{\min} and M_{map} . The critical temperature T_c , scaling dimension Δ_σ , and critical exponent ν , along with their standard errors, are estimated via finite-size scaling within the interval $T \in (0.840, 0.966)$ with step size $\Delta T = 0.002$. Theoretical values from the literature are included for comparison and the values of Δ_σ and ν marked with * are without higher-order corrections.

numerical value of $\nu = 0.722$ and $\Delta_\sigma = 0.128$ [56], which validates that all of these observables could serve as alternative order parameters. With the FSS procedure [55], we locate the critical temperature and extract the critical exponents for all these order parameters as detailed in Tab. II. They agree with the existing numerical values very well. We conclude that all occupancies of these states along with the magnetization-like quantity M_{map} can serve as alternative order parameters for $q = 4$ Potts model as well.

IV. CONCLUSION

Through systematic finite-size scaling analyses, we have discovered and validated a family of alternative order parameters for the square-lattice $q = 3$ and $q = 4$ Potts models. These include: (1) the conventional order parameter based on dominant spin state occupancy, (2) novel parameters derived from secondary and minimal spin states, and (3) magnetization-like quantities emerging from reduced representations with only two spin components. We have rigorously established the intrinsic relationships between these alternative order parameters, demonstrating that they collectively provide multiple consistent characterizations of critical behavior. This unified framework explains the remarkable generalizability of Ising-trained machine learning models to Potts systems. The models remain effective because criticality is redundantly encoded in these various order parameters, persisting even when explicit spin state information is partially lost through representation reduction.

Our findings suggest these novel order parameters generalize to other q -state Potts models, different lattice geometries (e.g., triangular or 3D), and systems with extended interactions (anti-ferromagnetic couplings, next-nearest neighbors). They may further enable studies of real-time dynamics or non-equilibrium phase transitions. Crucially, this work bridges machine learning's empirical success in phase classification with fundamental thermodynamic quantities, demonstrating that conventional order parameters are not unique descriptors of critical phenomena. Future

work could explore these generalizations systematically or analyze how neural networks leverage such order parameters across diverse spin systems.

ACKNOWLEDGMENTS

Y.D. thanks Ke Xu for the assistance with the usage of HPC in the cluster. This work is supported by the University of Bergen through “Akademikaavtalen” (K.T. and N.S.), the Taishan Scholars Program under Grant No. TSQNZ20221162, and the Shandong Excellent Young Scientists Fund Program (Overseas) under Grant No. 2023HWYQ-106 (Y.D.). Y. D. thanks the support from the cluster in FIAS and the Norwegian e-infrastructure UNINETT Sigma2 with Project Nos. NS9753K and NN9753K for the HPC resources and data storage in Norway. The work of N.S. was done at FIAS, supported by the AI grant at FIAS of SAMSON AG.

Appendix A: Finite-size scaling of alternative order parameters

1. $q = 3$ Potts model on a square lattice

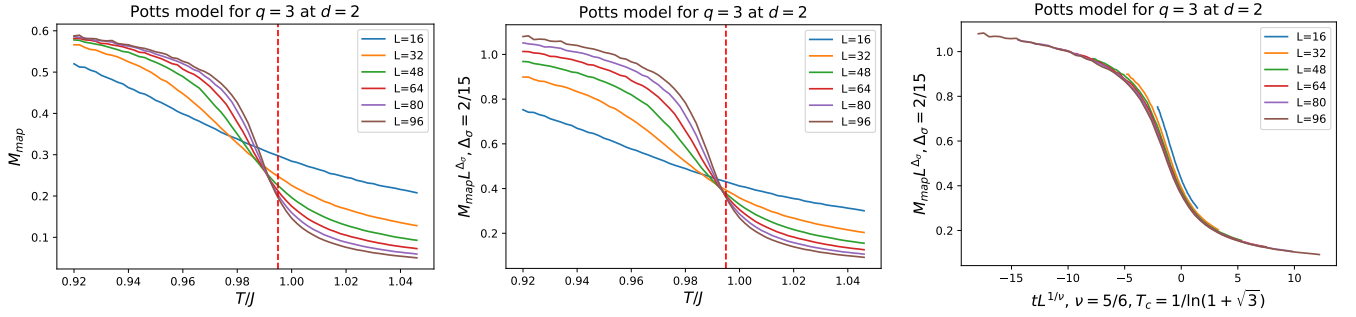


FIG. A1. (Color online) (Left) Order parameter M_{map} as a function of temperature T for the $q = 3$ Potts model on a square lattice with six different system sizes L . (Middle) Scaled order parameter $M_{\text{map}} L^{\Delta_\sigma}$ versus T , with curves intersecting near the theoretical critical temperature T_c , marked by the red vertical dashed line. (Right) Scaled order parameter $M_{\text{map}} L^{\Delta_\sigma}$ against the rescaled temperature $tL^{1/\nu}$, demonstrating data collapse consistent with finite-size scaling.

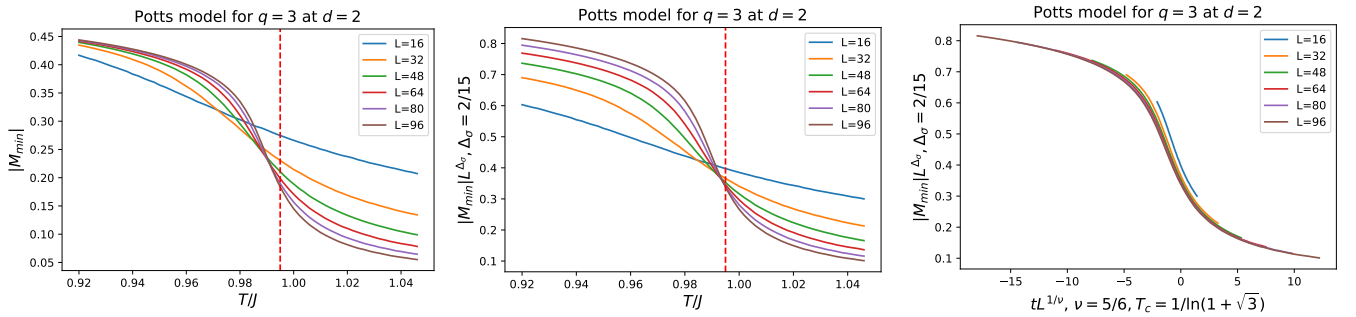


FIG. A2. (Color online) (Left) Order parameter M_{min} as a function of temperature T for the $q = 3$ Potts model on a square lattice with six different system sizes L . (Middle) Scaled order parameter $M_{\text{min}} L^{\Delta_\sigma}$ versus T , with curves intersecting near the theoretical critical temperature T_c , marked by the red vertical dashed line. (Right) Scaled order parameter $M_{\text{min}} L^{\Delta_\sigma}$ against the rescaled temperature $tL^{1/\nu}$, demonstrating data collapse consistent with finite-size scaling.

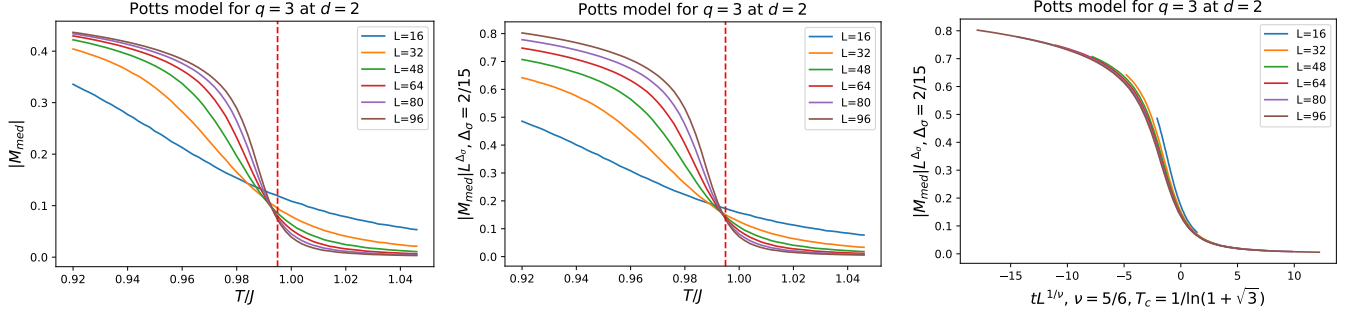


FIG. A3. (Color online) (Left) Order parameter M_{med} as a function of temperature T for the $q = 3$ Potts model on a square lattice with six different system sizes L . (Middle) Scaled order parameter $M_{\text{med}}L^{\Delta_\sigma}$ versus T , with curves intersecting near the theoretical critical temperature T_c , marked by the red vertical dashed line. (Right) Scaled order parameter $M_{\text{med}}L^{\Delta_\sigma}$ against the rescaled temperature $tL^{1/\nu}$, demonstrating data collapse consistent with finite-size scaling.

2. $q = 4$ Potts model on a square lattice

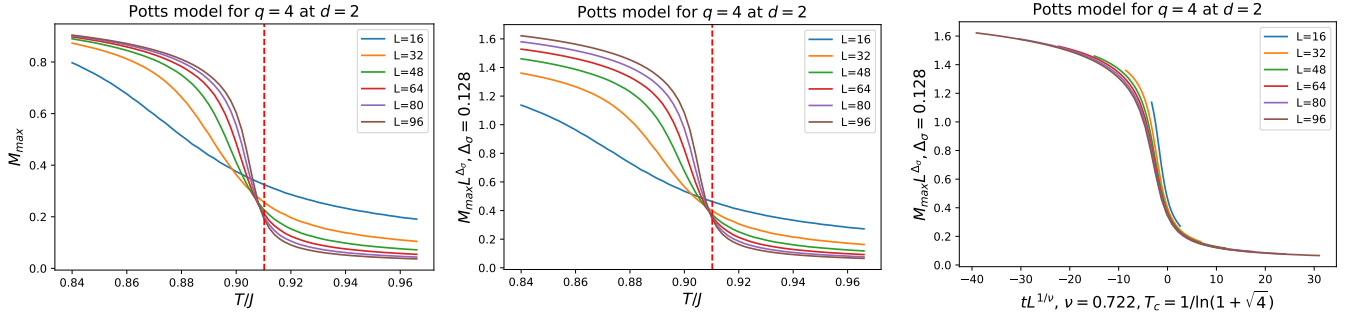


FIG. A4. (Color online) (Left) Order parameter M_{max} as a function of temperature T for the $q = 4$ Potts model on a square lattice with six different system sizes L . (Middle) Scaled order parameter $M_{\text{max}}L^{\Delta_\sigma}$ versus T , with curves intersecting near the theoretical critical temperature T_c , marked by the red vertical dashed line. (Right) Scaled order parameter $M_{\text{max}}L^{\Delta_\sigma}$ against the rescaled temperature $tL^{1/\nu}$, demonstrating data collapse consistent with finite-size scaling.

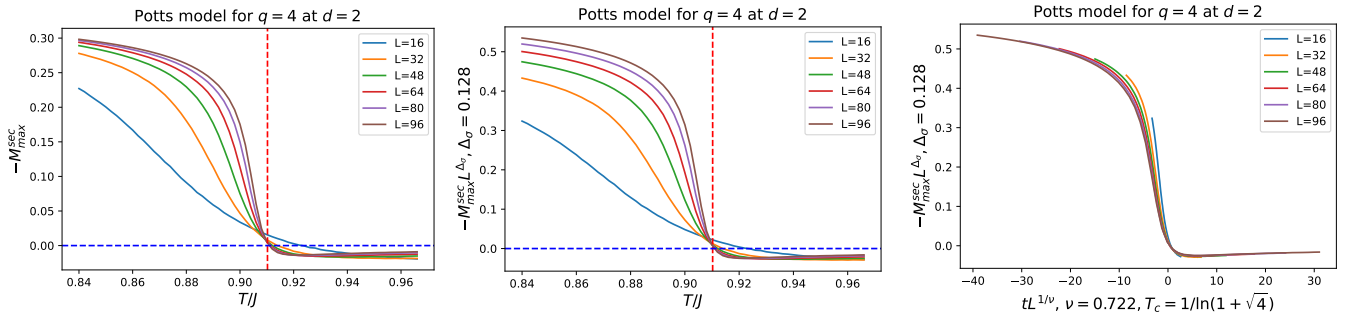


FIG. A5. (Color online) (Left) Order parameter $M_{\text{max}}^{\text{sec}}$ as a function of temperature T for the $q = 4$ Potts model on a square lattice with six different system sizes L . The blue horizontal dashed line marks zero to highlight the sign change. (Middle) Scaled order parameter $M_{\text{max}}^{\text{sec}}L^{\Delta_\sigma}$ versus T , with curves intersecting near the theoretical critical temperature T_c , marked by the red vertical dashed line. (Right) Scaled order parameter $M_{\text{max}}^{\text{sec}}L^{\Delta_\sigma}$ against the rescaled temperature $tL^{1/\nu}$, demonstrating data collapse consistent with finite-size scaling.

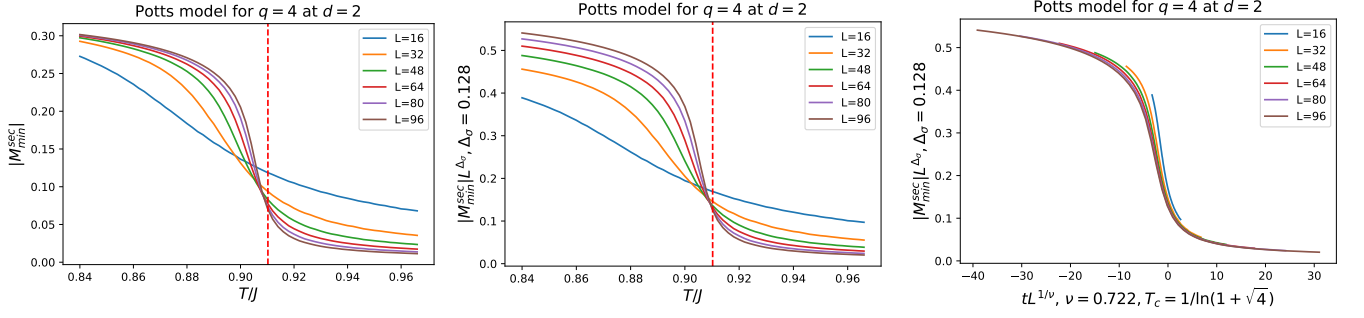


FIG. A6. (Color online) (Left) Order parameter M_{\min}^{sec} as a function of temperature T for the $q = 4$ Potts model on a square lattice with six different system sizes L . (Middle) Scaled order parameter $M_{\min}^{\text{sec}} L^{\Delta_\sigma}$ versus T , with curves intersecting near the theoretical critical temperature T_c , marked by the red vertical dashed line. (Right) Scaled order parameter $M_{\min}^{\text{sec}} L^{\Delta_\sigma}$ against the rescaled temperature $tL^{1/\nu}$, demonstrating data collapse consistent with finite-size scaling.

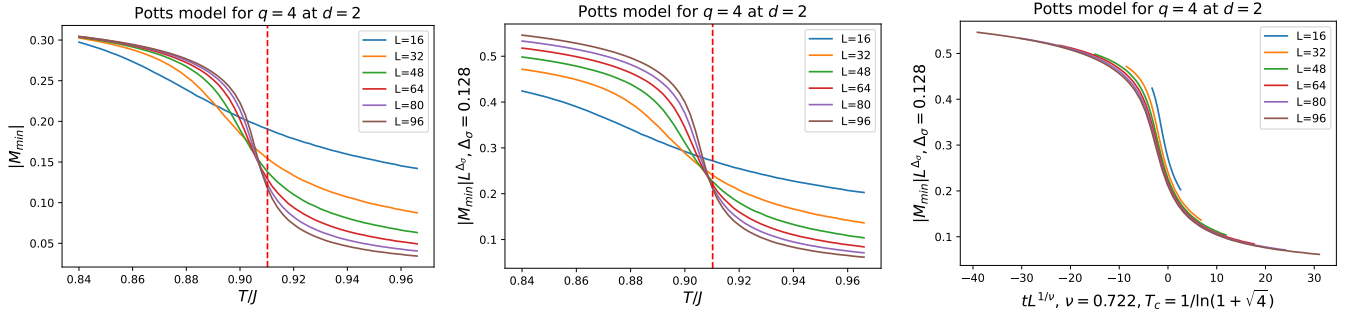


FIG. A7. (Color online) (Left) Order parameter M_{\min} as a function of temperature T for the $q = 4$ Potts model on a square lattice with six different system sizes L . (Middle) Scaled order parameter $M_{\min} L^{\Delta_\sigma}$ versus T , with curves intersecting near the theoretical critical temperature T_c , marked by the red vertical dashed line. (Right) Scaled order parameter $M_{\min} L^{\Delta_\sigma}$ against the rescaled temperature $tL^{1/\nu}$, demonstrating data collapse consistent with finite-size scaling.

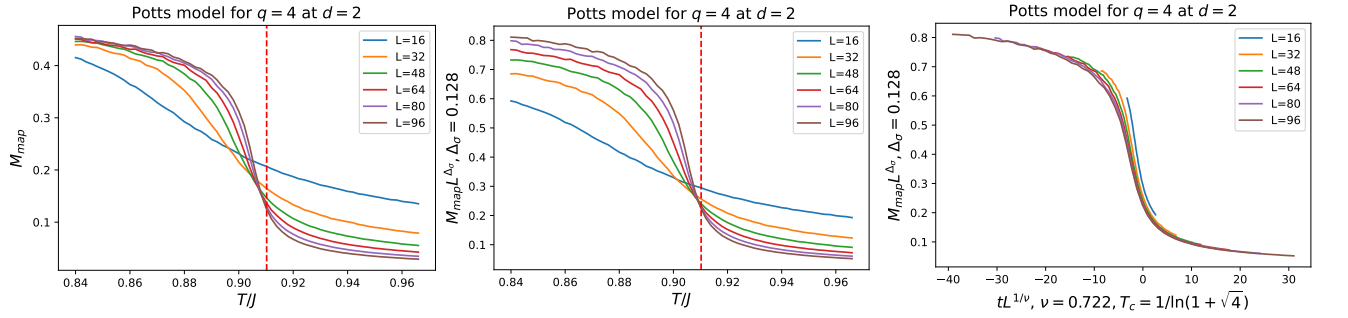


FIG. A8. (Color online) (Left) Order parameter M_{map} as a function of temperature T for the $q = 4$ Potts model on a square lattice with six different system sizes L . (Middle) Scaled order parameter $M_{\text{map}} L^{\Delta_\sigma}$ versus T , with curves intersecting near the theoretical critical temperature T_c , marked by the red vertical dashed line. (Right) Scaled order parameter $M_{\text{map}} L^{\Delta_\sigma}$ against the rescaled temperature $tL^{1/\nu}$, demonstrating data collapse consistent with finite-size scaling.

-
- [1] M. I. Jordan and T. M. Mitchell, Machine learning: Trends, perspectives, and prospects, *Science* **349**, 255 (2015).
 - [2] P. Mehta, M. Bukov, C.-H. Wang, A. G. Day, C. Richardson, C. K. Fisher, and D. J. Schwab, A high-bias, low-variance introduction to machine learning for physicists, *Phys. Rep.* **810**, 1 (2019).
 - [3] G. Carleo, I. Cirac, K. Cranmer, L. Daudet, M. Schuld, N. Tishby, L. Vogt-Maranto, and L. Zdeborová, Machine learning and the physical sciences, *Rev. Mod. Phys.* **91**, 045002 (2019).
 - [4] L. Wang, Discovering phase transitions with unsupervised learning, *Phys. Rev. B* **94**, 195105 (2016).
 - [5] E. P. Van Nieuwenburg, Y.-H. Liu, and S. D. Huber, Learning phase transitions by confusion, *Nat. Phys.* **13**, 435 (2017).
 - [6] S. J. Wetzel, Unsupervised learning of phase transitions: From principal component analysis to variational autoencoders, *Phys. Rev. E* **96**, 022140 (2017).
 - [7] W. Hu, R. R. Singh, and R. T. Scalettar, Discovering phases, phase transitions, and crossovers through unsupervised machine learning: A critical examination, *Phys. Rev. E* **95**, 062122 (2017).
 - [8] J. Carrasquilla and R. G. Melko, Machine learning phases of matter, *Nat. Phys.* **13**, 431 (2017).
 - [9] S. J. Wetzel and M. Scherzer, Machine learning of explicit order parameters: From the Ising model to SU(2) lattice gauge theory, *Phys. Rev. B* **96**, 184410 (2017).
 - [10] B. S. Rem, N. Käming, M. Tarnowski, L. Asteria, N. Fläschner, C. Becker, K. Sengstock, and C. Weitenberg, Identifying quantum phase transitions using artificial neural networks on experimental data, *Nat. Phys.* **15**, 917 (2019).
 - [11] X.-Y. Dong, F. Pollmann, X.-F. Zhang, *et al.*, Machine learning of quantum phase transitions, *Phys. Rev. B* **99**, 121104 (2019).
 - [12] W. Zhang, J. Liu, and T.-C. Wei, Machine learning of phase transitions in the percolation and XY models, *Phys. Rev. E* **99**, 032142 (2019).
 - [13] Y. Zhang, P. Ginsparg, and E.-A. Kim, Interpreting machine learning of topological quantum phase transitions, *Phys. Rev. Research* **2**, 023283 (2020).
 - [14] D. Boyda, M. N. Chernodub, N. Gerasimeniuk, V. Goy, S. Liubimov, and A. Molochkov, Finding the deconfinement temperature in lattice Yang-Mills theories from outside the scaling window with machine learning, *Phys. Rev. D* **103**, 014509 (2021).
 - [15] Y. Zhang and E.-A. Kim, Quantum loop topography for machine learning, *Phys. Rev. Lett.* **118**, 216401 (2017).
 - [16] P. Zhang, H. Shen, and H. Zhai, Machine learning topological invariants with neural networks, *Phys. Rev. Lett.* **120**, 066401 (2018).
 - [17] H. Araki, T. Mizoguchi, and Y. Hatsugai, Phase diagram of a disordered higher-order topological insulator: A machine learning study, *Phys. Rev. B* **99**, 085406 (2019).
 - [18] J. F. Rodriguez-Nieva and M. S. Scheurer, Identifying topological order through unsupervised machine learning, *Nat. Phys.* **15**, 790 (2019).
 - [19] G. Carleo and M. Troyer, Solving the quantum many-body problem with artificial neural networks, *Science* **355**, 602 (2017).
 - [20] K. Mills, P. Ronagh, and I. Tamblin, Finding the ground state of spin Hamiltonians with reinforcement learning, *Nat. Mach. Intell.* **2**, 509 (2020).
 - [21] C. Fan, M. Shen, Z. Nussinov, Z. Liu, Y. Sun, and Y.-Y. Liu, Searching for spin glass ground states through deep reinforcement learning, *Nat. Commun.* **14**, 725 (2023).
 - [22] T. Duric, J. H. Chung, B. Yang, and P. Sengupta, Spin-1/2 Kagome Heisenberg Antiferromagnet: Machine Learning Discovery of the Spinon Pair-Density-Wave Ground State, *Phys. Rev. X* **15**, 011047 (2025).
 - [23] L. Huang and L. Wang, Accelerated Monte Carlo simulations with restricted Boltzmann machines, *Phys. Rev. B* **95**, 035105 (2017).
 - [24] L. Wang, Exploring cluster Monte Carlo updates with Boltzmann machines, *Phys. Rev. E* **96**, 051301 (2017).
 - [25] T. Song and H. Lee, Accelerated continuous time quantum Monte Carlo method with machine learning, *Phys. Rev. B* **100**, 045153 (2019).
 - [26] S. Li, P. M. Dee, E. Khatami, and S. Johnston, Accelerating lattice quantum Monte Carlo simulations using artificial neural networks: Application to the Holstein model, *Phys. Rev. B* **100**, 020302 (2019).
 - [27] McNaughton, B and Milosević, M V and Perali, A and Pilati, S, Boosting Monte Carlo simulations of spin glasses using autoregressive neural networks, *Phys. Rev. E* **101**, 053312 (2020).
 - [28] Z. Tian, S. Zhang, and G.-W. Chern, Machine learning for structure-property mapping of Ising models: Scalability and limitations, *Phys. Rev. E* **108**, 065304 (2023).
 - [29] K. Kashiwa, Y. Kikuchi, and A. Tomiya, Phase transition encoded in neural network, *Prog. Theor. Exp. Phys.* **2019**, 083A04 (2019).
 - [30] Z. Li, M. Luo, and X. Wan, Extracting critical exponents by finite-size scaling with convolutional neural networks, *Phys. Rev. B* **99**, 075418 (2019).
 - [31] A. Abuali, D. A. Clarke, M. Hjorth-Jensen, I. Konstantinidis, C. Ratti, and J. Yang, Deep learning of phase transitions with minimal examples, *arXiv preprint arXiv:2501.05547* (2025).
 - [32] D. Kim and D.-H. Kim, Smallest neural network to learn the Ising criticality, *Phys. Rev. E* **98**, 022138 (2018).
 - [33] T. Westerhout, N. Astrakhantsev, K. S. Tikhonov, M. I. Katsnelson, and A. A. Bagrov, Generalization properties of neural network approximations to frustrated magnet ground states, *Nat. Commun.* **11**, 1 (2020).

- [34] I. Corte, S. Acevedo, M. Arlego, and C. Lamas, Exploring neural network training strategies to determine phase transitions in frustrated magnetic models, *Comput. Mater. Sci.* **198**, 110702 (2021).
- [35] C.-D. Li, D.-R. Tan, and F.-J. Jiang, Applications of neural networks to the studies of phase transitions of two-dimensional Potts models, *Annals of Physics* **391**, 312 (2018).
- [36] X. Zhao and L. Fu, Machine learning phase transition: An iterative proposal, *Annals of Physics* **410**, 167938 (2019).
- [37] D.-R. Tan, C. Li, W.-P. Zhu, and F.-J. Jiang, A comprehensive neural networks study of the phase transitions of Potts model, *New J. Phys.* **22**, 063016 (2020).
- [38] D. Giataganas, C.-Y. Huang, and F.-L. Lin, Neural network flows of low q -state Potts and clock models, *New J. Phys.* **24**, 043040 (2022).
- [39] A. Tirelli, D. O. Carvalho, L. A. Oliveira, J. P. de Lima, N. C. Costa, and R. R. dos Santos, Unsupervised machine learning approaches to the q -state Potts model, *Euro. Phys. J. B* **95**, 189 (2022).
- [40] X. Chen, F. Liu, S. Chen, J. Shen, W. Deng, G. Papp, W. Li, and C. Yang, Study of phase transition of Potts model with Domain Adversarial Neural Network, *Phys. A: Stat. Mech. Appl.* **617**, 128666 (2023).
- [41] X. Chen, F. Liu, W. Deng, S. Chen, J. Shen, G. Papp, W. Li, and C. Yang, Applications of Domain Adversarial Neural Network in phase transition of 3D Potts model, *Phys. A: Stat. Mech. Appl.* **637**, 129533 (2024).
- [42] K. Shiina, H. Mori, Y. Okabe, and H. K. Lee, Machine-learning studies on spin models, *Sci Rep* **10**, 2177 (2020).
- [43] D. Bachtis, G. Aarts, and B. Lucini, Mapping distinct phase transitions to a neural network, *Phys. Rev. E* **102**, 053306 (2020).
- [44] K. Fukushima and K. Sakai, Can a CNN trained on the Ising model detect the phase transition of the q -state Potts model?, *Prog. Theor. Exp. Phys.* **2021** (2021), 061A01.
- [45] H. M. Yau and N. Su, On the generalizability of artificial neural networks in spin models, *SciPost Physics Core* **5**, 032 (2022).
- [46] Y.-H. Tseng and F.-J. Jiang, Learning the phase transitions of two-dimensional Potts model with a pre-trained one-dimensional neural network, *Results Phys.* **56**, 107264 (2024).
- [47] C. Vanderzande, Bulk and surface critical behaviour at the conformal invariant point in the Z_5 model, *J. Phys. A* **20**, L549 (1987).
- [48] H. A. Fernandes, E. Arashiro, J. D. de Felício, and A. Caparica, An alternative order parameter for the 4-state potts model, *Physica A* **366**, 255 (2006).
- [49] V. Beffara and H. Duminil-Copin, The self-dual point of the two-dimensional random-cluster model is critical for $q \geq 1$, *Probability Theory and Related Fields* **153**, 511 (2012).
- [50] H. Duminil-Copin, V. Sidoravicius, and V. Tassion, Continuity of the phase transition for planar random-cluster and potts models with $1 \leq q \leq 4$, *Communications in Mathematical Physics* **349**, 47 (2017).
- [51] H. Duminil-Copin, M. Gagnebin, M. Harel, I. Manolescu, and V. Tassion, Discontinuity of the phase transition for the planar random-cluster and potts models with $q > 4$, *arXiv preprint arXiv:1611.09877* (2016).
- [52] F.-Y. Wu, The Potts model, *Rev. Mod. Phys.* **54**, 235 (1982).
- [53] R. H. Swendsen and J.-S. Wang, Nonuniversal critical dynamics in Monte Carlo simulations, *Phys. Rev. Lett* **58**, 86 (1987).
- [54] D. J. Sharpe, [Swendsen-Wang algorithm for Potts model](#) (2018).
- [55] O. Melchert, [autoScale.py-A program for automatic finite-size scaling analyses: A user's guide](#), *arXiv preprint arXiv:0910.5403* (2009).
- [56] J. Salas and A. D. Sokal, Logarithmic corrections and finite-size scaling in the two-dimensional 4-state Potts model, *J. Stat. Phys* **88**, 567 (1997).